

Integration of constructal distributors to a mini crossflow heat exchanger and their assembly configuration optimization

Lingai Luo^{a,*}, Yilin Fan^a, Weiwei Zhang^b, Xigang Yuan^b, Noël Midoux^c

^aLaboratoire Optimisation de la Conception et Ingénierie de l'Environnement (LOCIE), Université de Savoie, Campus Scientifique, Savoie Technolac, 73376 Le Bourget-Du-Lac cedex, France

^bChemical Engineering Research Center, Tianjin University, Tianjin 300072, People's Republic of China

^cLaboratoire des Sciences du Génie Chimique du CNRS, BP451 ENSIC-INPL 1 rue Grandville, Nancy F54001, France

Received 10 October 2006; received in revised form 7 February 2007; accepted 13 February 2007

Available online 27 March 2007

Abstract

In this paper, the idea of coupling constructal distributors/collectors with a mini crossflow heat exchanger (MCHE) to solve the problem of flow maldistribution is presented. After a brief description of the design and scaling laws of the constructal distributor, experimental and simulation results have been discussed to investigate relations among flow distribution, heat transfer and pressure drop. It is shown that the introduction of constructal distributors and/or collectors could improve the quality of fluid distribution and consequently lead to heat transfer intensification of the MCHE, but it also results in higher pressure drops. Different assembly configurations involving distributor, heat exchanger and collector have also been compared. The configuration where the inlet is equipped with a conventional pyramid distributor and the outlet is equipped with a constructal collector (Apec) shows a relatively higher thermal performance as well as low pressure drops in our cases considered. © 2007 Elsevier Ltd. All rights reserved.

Keywords: Flow maldistribution; Constructal distributor; Mini crossflow heat exchanger (MCHE); Thermal performance; Pressure drop; Assembly configuration

1. Introduction

Heat exchangers, as typical process and chemical engineering units, are widely used in different aspects of industry. Nowadays, the demand for highly efficient heat exchangers such as compact heat exchangers has started increasing as a result of the diminishing world energy resources and increasing energy cost, which then stimulates the diversification of heat transfer intensification methods. However, a large part of these methods, either active or passive, is restricted to create extended useful heat transfer surfaces or to generate turbulence flow to increase the overall heat transfer coefficient. The deterioration in the performance of heat exchangers due to *flow maldistribution* should also be an important issue. In most design of heat exchangers, it is assumed that the flow is uniformly distributed over different channels or tubes, but under operating condition in real-world engineering, this assumption is questionable.

A lot of related research works (Fleming, 1967; Chiou, 1978, 1980; Lalot et al., 1999; Ranganayakulu and Seetharamu, 1999a,b; Bobbili et al., 2002, 2006; Yuan, 2003; Jiao et al., 2003; Wen and Li, 2004; Jiao and Baek, 2005; Srihari et al., 2005) have proved that flow maldistribution reduces significantly the idealized heat exchanger performance especially in mini-scale heat exchangers and finding effective methods to solve this problem is a real challenge faced by researchers and engineers.

Besides the passage-to-passage maldistribution (Mueller and Chiou, 1988) which occurs within highly compact heat exchanger because of its manufacturing tolerances, fouling, condensable impurities, etc., more and more studies are focused on decreasing the gross maldistribution, which is mainly associated with improper design of distributor and/or collector configuration. Dispersion models have been proposed to describe the effect of flow maldistribution in shell-and-tube heat exchangers (Xuan and Roetzel, 1993; Roetzel and Ranong, 1999; Sahoo and Roetzel, 2002), finned tube heat exchangers (Aganda et al., 2000), plate heat exchangers (Roetzel and Das, 1995;

* Corresponding author. Tel.: +33 4 79 75 81 93; fax: +33 4 79 75 81 44.
E-mail address: Lingai.LUO@univ-savoie.fr (L. Luo).

Luo and Roetzel, 2001; Gut et al., 2004; Srihari et al., 2005), other cross-flow-type heat exchangers (Luo and Roetzel, 1998; Ranganayakulu and Seetharamu, 1999a; Lalot et al., 1999), etc. Various methods have been suggested in order to obtain a uniform inlet flow distribution. Some of these consists in adding “packings” that are random at small scales, but regular at the larger scales, such as a uniformly perforated grid (Lalot et al., 1999), a baffle (Wen and Li, 2004; Wen et al., 2006) or a second header (Jiao et al., 2003), resulting in a higher pressure drop and flow dispersion that are undesirable from the engineering point of view. Others include modifying the corrugation angles or geometrical dimension of the distributor (Lalot et al., 1999; Jiao and Baek, 2005; Bobbili et al., 2006) to improve the quality of flow distribution.

In fact, properties expected from a “good” distributor are equidistribution of the flow rate (uniform irrigation), minimal dispersion, minimal void volume and minimal pressure drop, leading necessarily to some compromise. This problem cannot be solved by conventional ways but may be approached using multi-scale optimization methodology such as the so-called “constructal approach”, developed by Bejan and his co-workers from 1996 on, a quite general theory of multi-scale shapes and structures in nature and engineering (Bejan, 1997; Bejan and Tondeur, 1998). Details of the constructal approach may be found in Bejan (2000a) and in the book “Shape and Structure: from Engineering to Nature” (Bejan, 2000b). In “constructal” terms, the distributor or collector problem is topologically one of the connections between a point and a surface. The “point” is here the single inlet tube or pore, and the surface is the domain that must be fed by the distributed flow. The architecture for multi-objective systems that optimally distributes dissipation in time, space, scales and structure could be generated using constructal approach under specified constraints and duties (Luo et al., 2006).

The main objective of this paper is to present the idea of coupling constructal distributors/collectors with a heat exchanger to improve its thermal performance by solving the flow maldistribution problem. This work starts from the earlier work of Tondeur and Luo (2004) and Luo and Tondeur (2005a,b). Novel constructal distributors were designed and optimized by constructal approach and integrated to a MCHE. We first attempt to characterize distributors per se, that is, independently of the operation to which it will be attached. Then, numerical and experimental results are discussed in order to investigate the effect of constructal distributor/collector on the fluid equidistribution in the core of the MCHE, as well as its thermal performance and pressure drop. Clearly, there cannot be a unique correspondence between the global flux transferred and the quality of flow distribution, but a significant correlation should be possible between the effect of operating parameters (flow rates and temperatures) on the flux transferred on one hand, and an overall characteristic of the flow distribution on the other hand, a relation between variances for example. The parameters of useful pressure drop and lost pressure drop are defined to establish the relationships between the location of constructal component and the effect of flow equidistribution, and to the optimization of distributor/collector and heat exchanger as-

sembly configuration. Finally, conclusions and future work are summarized.

2. Branched fluid distributor: design and scaling laws

Let us first describe the constructal distributor of Fig. 1. Branched distributor based on a so-called “dichotomic tree” and optimized by constructal approach was designed and manufactured by laser polymerization stereolithography (André and Corbel, 1994). The structure of this distributor is determined by an optimization criterion that specifies the total flow rate and accounts for both viscous dissipation and total pore volume. The design guidelines and detail optimization procedure by constructal approach could be found in Tondeur and Luo (2004) and Luo and Tondeur (2005a), and it will be instructive to briefly restate key scaling laws and some useful conclusions already arrived.

The pore space of the distributor has the structure of a sequence of eight generations of T- or Y-bifurcations or divisions. It has a branching logic in which every channel is divided into two smaller branches; the number of the smallest channels thus generated is 2^m where m is the number of levels of branching, or “generations”. The number of channels that such a distributor can feed is therefore a power of 2 as $m = 0$ for the inlet channel. Since there are eight generations of bifurcations, there are $2^8 = 256$ final outlet channels.

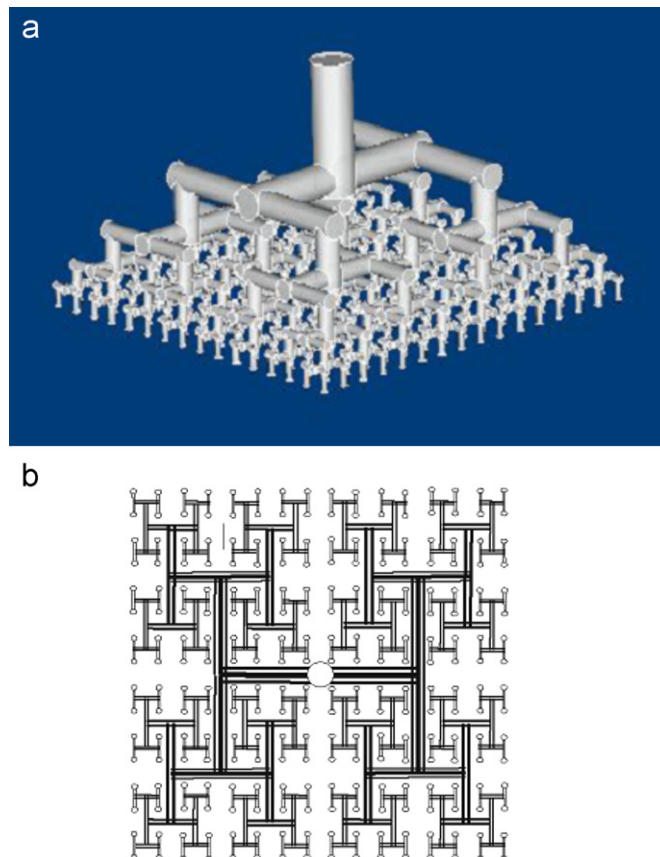


Fig. 1. Binary-branched fluid distributor. (a) Pore structure; (b) projection of pore network on base plane.

Number of pores n for any generation of index k :

$$n_k = 2^k. \quad (1)$$

Number of end points N (outlet ports) for m generations:

$$N = 2^m. \quad (2)$$

Scaling laws for channel lengths l :

$$l_k = \frac{L}{2^{(k+2)/2}} \text{ if } k \text{ even; } \quad l_k = \frac{L}{2^{(k+3)/2}} \text{ if } k \text{ odd,} \quad (3)$$

$$\frac{l_k}{l_{k+2}} = 2. \quad (4)$$

Channel length l is entirely determined by the overall size of the distributor (length of the side of the square L) and the constraint of uniform outlet distribution. No other consideration is introduced, and in particular, the length distribution is fully independent of the pore radii.

Total “horizontal” path length from inlet to outlet, with m even:

$$l_{\text{tot}} = \sum_{k=1}^{k=m} l_k = L[1 - 2^{-m/2}] \approx 0.94L (m = 8). \quad (5)$$

It clearly converges towards L when m increases.

Scaling laws for pore radii r , fluid velocity u and flow rate f in single pore (Hagen–Poiseuille type on laminar flow):

$$\left(\frac{r_k}{r_{k+1}}\right)^6 = 4 \quad \text{or} \quad \frac{r_k}{r_{k+1}} = \frac{u_k}{u_{k+1}} = \left(\frac{f_k}{f_{k+1}}\right)^{1/3} = 2^{1/3} \approx 1.26. \quad (6)$$

Scaling laws for relative overall dissipation D :

$$\left(\frac{D_k}{D_{k+1}}\right) = 2^{2/3} > 1 \text{ if } k \text{ even;} \quad \left(\frac{D_k}{D_{k+1}}\right) = 2^{-1/3} < 1 \text{ if } k \text{ odd} \quad (7)$$

$$\left(\frac{D_k}{D_{k+2}}\right) = 2^{1/3} > 1. \quad (8)$$

The factor $2^{1/3}$ is sometime referred to as Murray’s law. It is obtained by the optimization of the channel size distribution with an objective function of a combination of power dissipation and pore volume.

It is theoretically assumed that perfect flow distribution could be ensured, as the 256 paths are geometrically identical. In particular, their total lengths and the diameter distribution along the lengths are strictly the same. Fast camera pictures (Luo and Tondeur, 2005a) of the invasion experiment by a fluid carrying an optical tracer proved that flow equidistribution could be reached qualitatively at the outlet surface of this constructal distributor. However, these pictures also illustrate that there are a flow dispersion and a residence-time distribution, a departure from the ideal distribution (plug-flow type). We attribute this

maldistribution to two main reasons: on one hand, the imperfections and irregularities in fabrication, that is, the passage-to-passage maldistribution that cannot be avoided due to the manufacture accuracy limitation; on the other hand, direction changes and splitting such as in joint and elbows; the presumption of Poiseuille’s law is not obeyed because of perturbation and spiral vortex.

A number of formulations of the optimization problem also exist, surely leading to different scaling laws and different structures using similar principle in order to gain geometric degrees of freedom, and robustness with respect to possible pathologies.

3. Coupling constructal distributors with a heat exchanger

As mentioned above, an often hidden problem in running a heat exchanger is the uneven flow distribution that deteriorates its performance. Our objective is to develop a test for flow characterization to prove that the introduction of constructal distributors/collectors is more performing than what was done so far. The work starts with the MCHE, on which inlets and outlets for the two fluids may be equipped or not with constructal distributors/collectors (modified evolution of the structure shown in Fig. 1, which has seven generations of scales and 128 outlet ports corresponding to the surface of the MCHE instead of 256 outlet ports). Measuring both pressure drop and thermal flux transferred gives the global impact on its performance.

3.1. Cubic mini crossflow heat exchanger

The MCHE presented here is a simple and representative heat exchanger example suitable for the experimental test of thermal transfer. It was manufactured in the “Laboratoire des Sciences du Génie Chimique” (LSGC), a laboratory of the ENSIC-group in Nancy, by drilling two perpendicular sets of channels with a length of 56.5 mm in a cubic solid block of aluminum. In this exchanger, each set of channels is composed of 16 rows and 8 columns, the total number of channels thus being 128, all with a diameter of 2.5 mm. The two sets of channels are devoted, respectively, to cold and hot fluid, and both fluids are unmixed. Fig. 2 shows a schematic view of this exchanger.

The useful volume (V) of this exchanger is $56.5 \text{ mm} \times 56.5 \text{ mm} \times 56.5 \text{ mm}$, that is, $1.80 \times 10^{-4} \text{ m}^3$. The heat exchange surface area (A) ($5.68 \times 10^{-2} \text{ m}^2$) is calculated of all the tubes for one fluid. As a result the surface area density β (m^2/m^3), also called the compactness in other literatures, is about $316 \text{ m}^2/\text{m}^3$.

3.2. Constructal distributor versus conventional pyramid distributor

New constructal distributors were designed corresponding to the inlet or outlet surface and channel geometry of the MCHE. Polymer prototypes (Fig. 3) were manufactured in the “Département de Chimie-Physique des Réactions” (DCPR), a laboratory of the ENSIC-group in Nancy, using stereolithography technique. There are seven generations of bifurcations, final

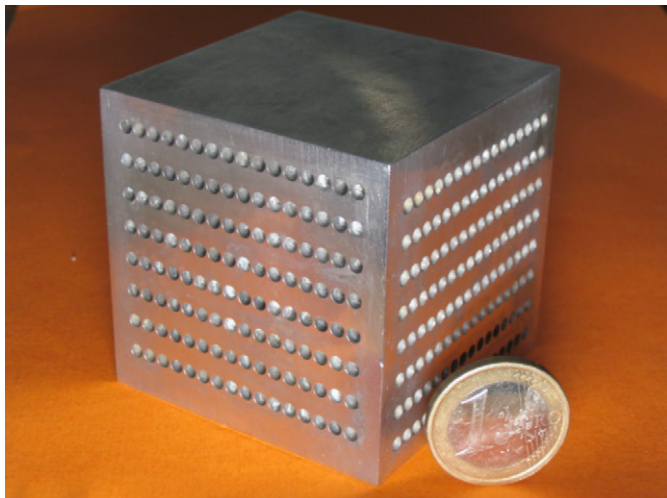


Fig. 2. Cubic MCHE in aluminum and a coin of 1 euro.

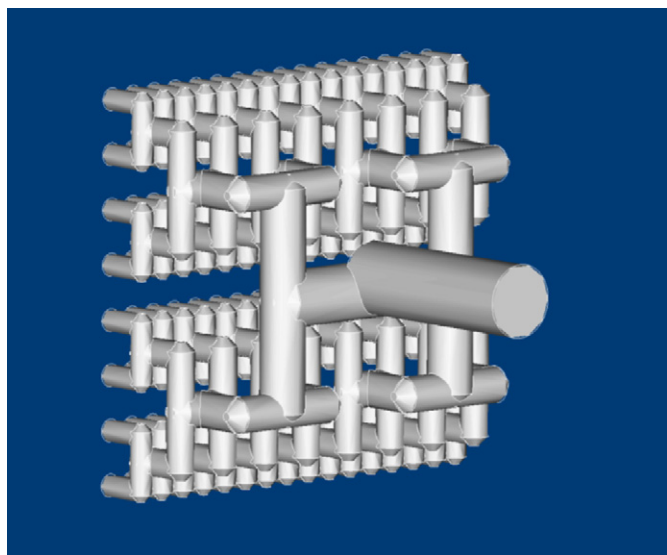


Fig. 3. Structure and geometrical dimensions of the constructal distributor with 7 scales and 128 outlets. The side of the square is 56.5 mm.

outlet channels being $2^7 = 128$, corresponding to the inlet or outlet surfaces of the MCHE. The resulting channels are indexed from 0 to 7, including the inlet channel (index 0). The latter is split perpendicularly into two opposing channels (index 1), and each of these is again split into two channels (index 2), such that channels of indices 1, 2 and 3 are coplanar (differentiate from Fig. 1 which has channels of indices 1 and 2 coplanar). The ends of pores 3 are elbows (downcomers), which descend into two new planes successively, containing pores of indices 4 and 5 in one plane and pores of indices 6 and 7 in the other.

Starting from the diameter of the smallest channels, $k = 7$, $d_7 = 2.5$ mm, which is identical to the channel diameter of the MCHE, we have $d_6 = d_7 = 2.5$ mm; $d_5 = 2.5 \times 1.26 = 3.15$ mm; $d_4 = d_3 = 3.15 \times 1.26 = 4$ mm; $d_2 = 4 \times 1.26 = 5$ mm; $d_1 = 5 \times 1.26 = 6.3$ mm; $d_0 = 6.3 \times 1.26 = 8$ mm. The factor 1.26 ($2^{1/3}$), which is approximately applied to determine the channel

diameters, obeys the same scaling law presented in the former section.

Conventional pyramid distributors (Fig. 4), which were also manufactured in DCPR, are introduced for comparison. They have the same external dimensions as the constructal distributors, but instead of the bifurcated interior structure, they show a simple pyramidal space from one inlet tube to a square surface.

3.3. Different assembly configurations

In order to estimate the effect of flow distribution that is associated with the sort of inlet distributor or outlet collector or both, assembly configuration optimization should be done with the criteria of better thermal performance and reasonable pressure drop. Here, we propose four assembly configurations of distributors/collectors connected with the MCHE, differentiated by the location of the constructal components:

- Acep: constructal inlet–exchanger–pyramidal outlet;
- Apec: pyramidal inlet–exchanger–constructal outlet;
- Acec: constructal inlet–exchanger–constructal outlet;
- Apep: pyramidal inlet–exchanger–pyramidal outlet.

Within our cases, the same assembly configurations were used for both fluids, hot and cold. For example, if an inlet constructal distributor and an outlet conventional pyramid collector were employed for the cold side of the MCHE (Acep), then the same configuration Acep was used for the hot side. The tested model that was formed by the distributor, the MCHE and the collector was then integrated and insulated by heat-barrier materials to avoid heat losses.

We choose the pure laminar flow conditions in our test as it has been theoretically shown that laminar flows can provide high heat transfer coefficients under a reasonable pressure drop in mini heat exchangers. Another reason lies in the thermal restriction of the materials. In fact, the photosensitive epoxy resin (RP Cure 400 AR) used has a melting or softening temperature of about 50°C . In order to prevent deformation of these distributors and to maintain a reasonable temperature difference between hot water and cold water, two thermostats with limited maximum flow rate were employed to maintain the hot water inlet temperature at about 30°C , and cold water inlet temperature at about $3\text{--}5^\circ\text{C}$. Numerical and experimental results will be presented in the following sections.

4. Experimental analysis

Experimental tests have been done in an installation composed of two independent leak tight loops with water as circulation fluids for both hot and cold sides, as shown in Fig. 5. On the hot side, the flow rate was fixed at 3.2×10^{-3} kg/s corresponding to a channel Reynolds number $Re = \rho v d / \mu$ of 363, a linear velocity of 0.12 m/s; the inlet temperature was about 30°C . On the cold side, the flow rate of cold water ranged from 20×10^{-3} to 100×10^{-3} kg/s, corresponding to Reynolds numbers from 50 to 260 and flow velocities ranging from 0.03

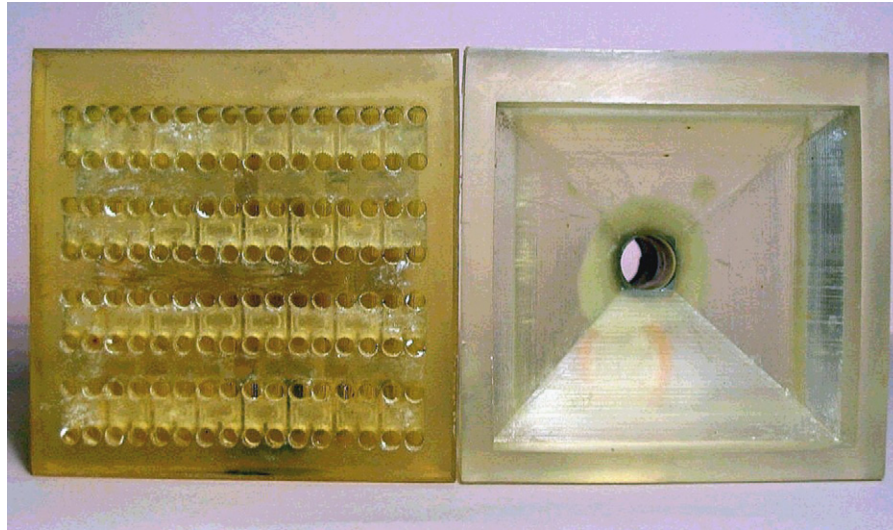


Fig. 4. Constructral distributor versus conventional pyramid distributor.

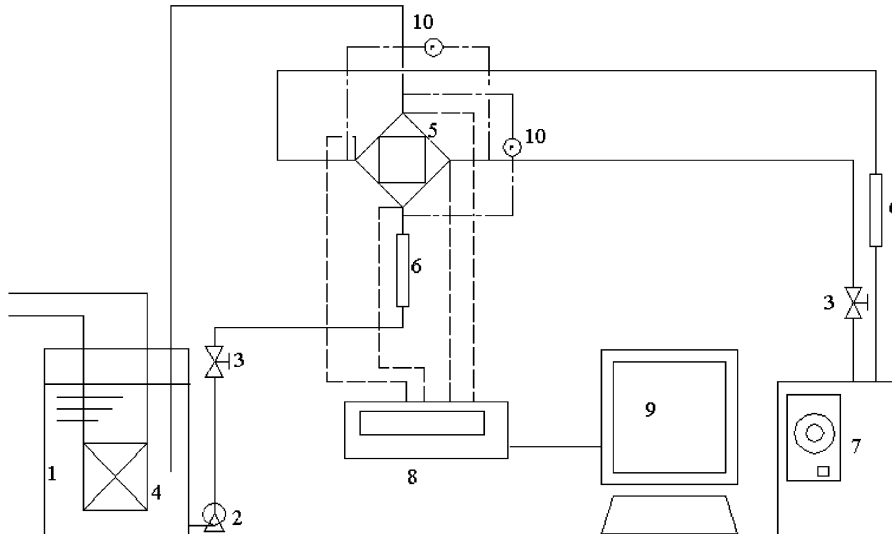


Fig. 5. Schematic diagram of experimental system. (1) Storage tank; (2) pump; (3) valve; (4) refrigerator; (5) tested model; (6) flowmeter; (7) thermostat; (8) temperature sensor; (9) computer; (10) manometer.

to 0.15 m/s, with the inlet temperature in the range of 3–5 °C. Inlet and outlet temperatures as well as pressure drops for both fluids were measured at different flow rates. For each set of flow rates, several measurements were taken and the energy balance was calculated. The uncertainty on the overall heat transfer coefficient from the uncertainty on the heat balance of the two fluids is less than 6.5%. The logarithmic mean temperature difference method (LMTD) is used to evaluate the heat transfer power q , the overall heat transfer coefficient U and the pressure drop Δp of different assembly configurations.

$$q = U A F \Delta T_m. \quad (9)$$

Here, F is the LMTD correction factor. Considering the specific geometry and flow arrangement of the MCHE, it approaches 1 in our cases (Hewitt, 1992).

The mean temperature difference ΔT_m is calculated by the formula

$$\Delta T_m = \frac{(T_{\text{hot,in}} - T_{\text{cold,out}}) - (T_{\text{hot,out}} - T_{\text{cold,in}})}{\ln(T_{\text{hot,in}} - T_{\text{cold,out}} / T_{\text{hot,out}} - T_{\text{cold,in}})}. \quad (10)$$

4.1. Overall heat transfer coefficient

From Fig. 6, it is evident that the overall heat transfer coefficients of the configurations that involve constructral distributors/collectors (Acec, Acep and Apec) are higher than that of the configuration Apep. That is to say, the thermal performance of the MCHE represented by U is improved by the introduction of the constructral components. This is not quite surprising and the results are in correspondence with the presumption that the constructral distributors can to some extent equalize the fluid

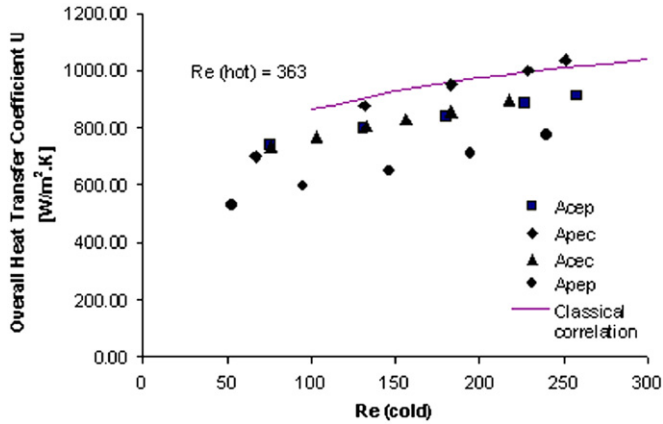


Fig. 6. Overall heat transfer coefficient U versus channel Re .

distribution and consequently lead to the thermal performance improvement of the MCHE.

Acec and Acep have approximately equal effects, and compared to Apep, the overall heat transfer coefficient of the MCHE is increased from 30% to 15% when the Re increases from 50 to 260. From these observations, it would seem that if a constructal distributor has been introduced in the inlet of the MCHE, the fluid distribution is improved to the point that the employment of a constructal collector in the outlet is not necessary, since it would only increase the pressure drop of the system (to be discussed later).

From Fig. 6, one also notices that it is the Apec with a conventional pyramid inlet distributor and a constructal outlet collector that performs best. On maximum condition, the difference of U between Apec and Acec is about 10%; the difference of U between Apec and Apep is of 28%. The remarkable point why Apec performs better than Acec will be further discussed later in this paper.

4.2. Nusselt numbers

For a better understanding of the function of the constructal components in the heat transfer process, a classical correlation proposed by Seider and Tate (1936) is introduced to calculate the Nusselt numbers and theoretical heat transfer coefficient of the MCHE, as shown in Fig. 6. This correlation calculates the theoretical overall heat transfer coefficient with the assumption that the flow is uniformly distributed over the different channels.

$$Nu = 1.86(Re)^{1/3} \left(Pr \frac{d}{l} \right)^{1/3} \left(\frac{\mu}{\mu_w} \right)^{0.14}, \quad (11)$$

$$\frac{1}{U} = \frac{1}{h_{hot}} + \frac{\delta}{k} + \frac{1}{h_{cold}}. \quad (12)$$

With $Re = 100 \sim 2100$; $l/d > 60$; $Re Pr(d/l) > 10$.

Note that the conduction resistance of the MCHE depends on the thermal conductivity of the material and the internal geometry of the MCHE. We chose an equivalent wall thickness in the calculation of this resistance and it shows that the

Table 1

Nu correlations for different assembly configurations

Assembly configuration	Correlation	Max. error (%)
Acep	$Nu = 1.87(Re)^{0.312} (Pr \frac{d}{l})^{1/3} (\frac{\mu}{\mu_w})^{0.14}$ (13)	2.2
Apec	$Nu = 0.72(Re)^{0.504} (Pr \frac{d}{l})^{1/3} (\frac{\mu}{\mu_w})^{0.14}$ (14)	1.2
Acec	$Nu = 1.45(Re)^{0.358} (Pr \frac{d}{l})^{1/3} (\frac{\mu}{\mu_w})^{0.14}$ (15)	1.8
Apep	$Nu = 0.97(Re)^{0.394} (Pr \frac{d}{l})^{1/3} (\frac{\mu}{\mu_w})^{0.14}$ (16)	4.6
Ideal condition	$Nu = 1.86(Re)^{1/3} (Pr \frac{d}{l})^{1/3} (\frac{\mu}{\mu_w})^{0.14}$ (11)	

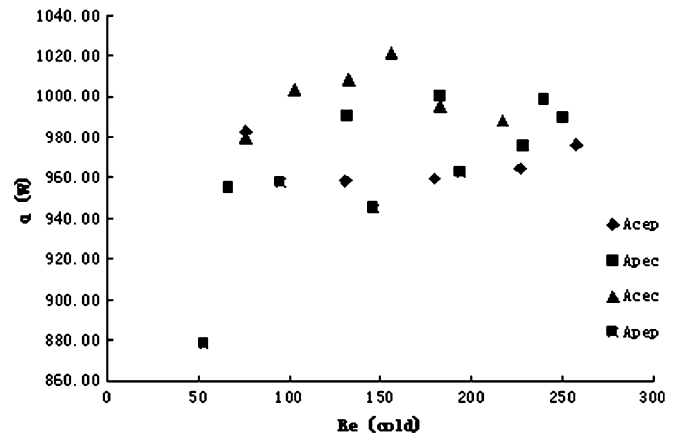


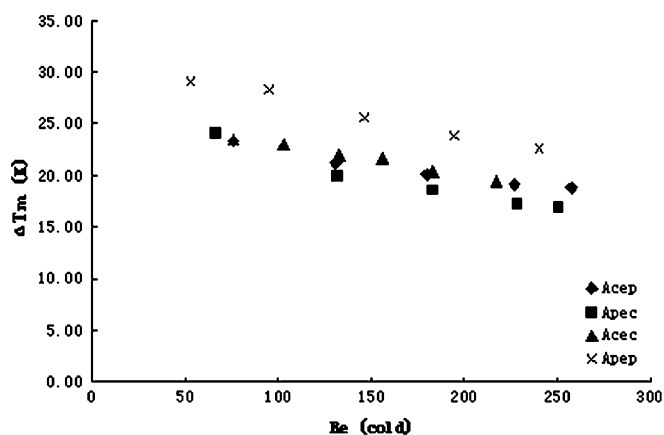
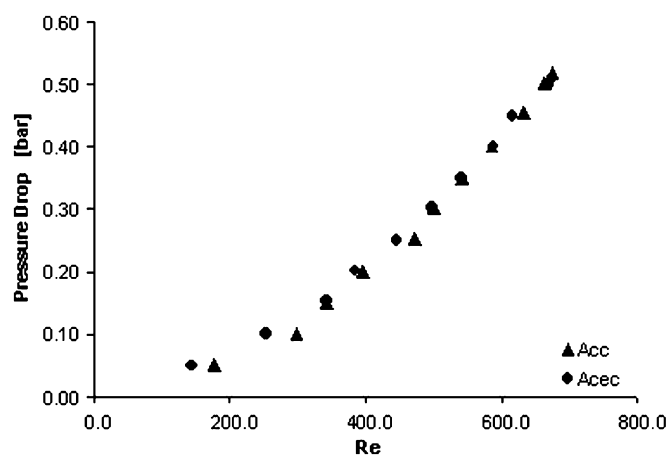
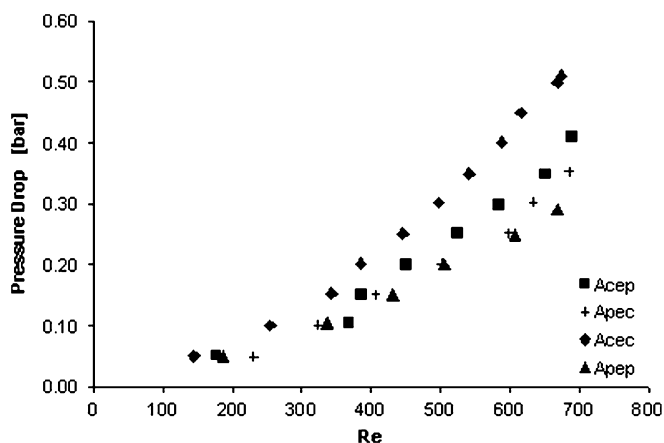
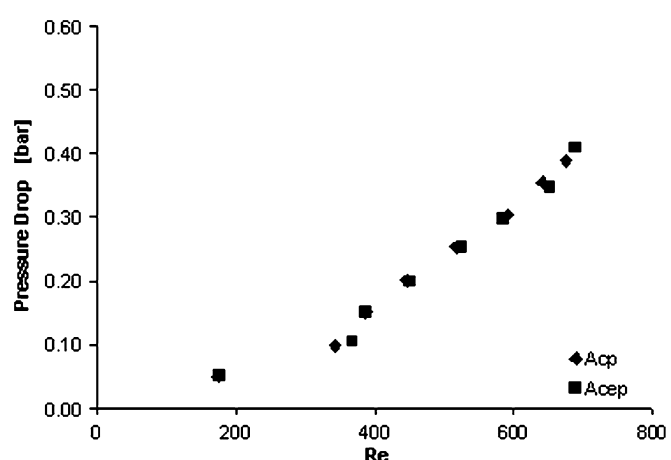
Fig. 7. Heat transfer power for different configurations.

conduction resistance is neglectable ($< 2\%$) with regard to the convection resistance in our study conditions. However in micro- or meso-scale heat exchangers, there could be a longitudinal conductivity problem. It tends to homogenize the temperature in the exchanger, thus reducing the temperature gradient responsible for the temperature switch. Related researches have been done by Luo et al. (2000, 2001). Detail discussion of this problem is not extended in the present article, but it will be paid attention to in our future work.

Fitting curves are also calculated with the same form of Seider and Tate correlation, using the experimental data of different configurations. The correlations for Nusselt numbers and the uncertainty are listed in Table 1. The experimental data of overall heat transfer coefficient U of different configurations is fitted quite well with only small error occurring (less than 5%).

4.3. Heat transfer power

Heat transfer power of the MCHE is shown in Fig. 7. Except that of Apep, it ranges from 940 to 1200 W with the Re from 50 to 260. Within our experimental conditions, the volumetric power of this MCHE is in the order of magnitude of 6000 kW/m^3 . However, The difference among assembly configurations is not apparent enough to reach a conclusion within the uncertainty considered. In fact, heat transfer is surely dependent on the flow rate and the LMTD. In laminar flow, the LMTD decreases as flow rate increases, as shown in Fig. 8,

Fig. 8. ΔT_m for different configurations.Fig. 10. Pressure drops of the pair Acc and Acec versus Re number.Fig. 9. Δp versus Re number with different configuration.Fig. 11. Pressure drops of the pair Acp and Acep versus Re number.

leading to an opposite way for heat transfer power increase. A noticeable feature in Fig. 8 is that the configuration Apep shows a great temperature difference between the fluid streams, which to a second law analysis point of view, also means a greater exergy loss during heat transfer procedure (Ahern, 1980). The range of Reynolds numbers studied in our experiment is so small that information of the heat transfer procedure in turbulence flow and the transitional flow cannot be gathered.

4.4. Pressure drop

With an increase in overall heat transfer coefficient, an increase in pressure drop also occurs. Series of tests were also carried out to examine the pressure drop between the inlet and outlet of different configurations. The property values for the density and viscosity were taken at 20 °C, since that was the temperature when the manometer readings were taken. Results are shown in Fig. 9.

From Fig. 9, it can be observed that the pressure drops increase greatly with Re number increases and relatively high

pressure drops have been measured (0.3–0.5 bar) at the channel Re number of 700. Meanwhile, the pressure drops of the configuration involving two constructal distributors (Acec) are consistently higher than those of the others in the considered Re range. For example, the pressure drop of Acec is 0.50 bar, 72.4% higher than that of Apep (0.29 bar) with the same Re of 690. The clearly more pronounced pressure drops in Acec are mainly attributable to the internal structure complexity of the constructal components.

To evaluate separately the contributions of these components on the pressure drops, comparative experiments have been carried out with the inlet and outlet pieces alone, without the MCHE.

Analyzing the four figures (Figs. 10–13), one can find that the difference of the pressure drops with or without the MCHE can be neglected (approximately 0.05%) except for the pair App and Apep. It means that the MCHE has little impact on the pressure drop, when a constructal component is used as inlet distributor or outlet collector. Theoretical calculation can also prove that the pressure drops of the MCHE range from 2.0×10^{-4} to 8.1×10^{-4} bar with the following classical equation (Holman,

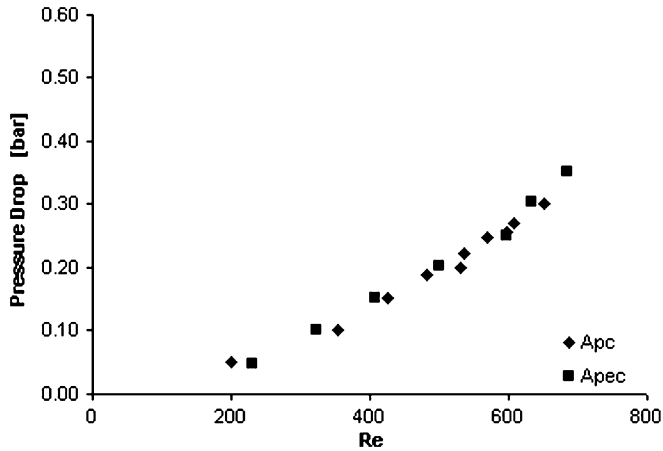
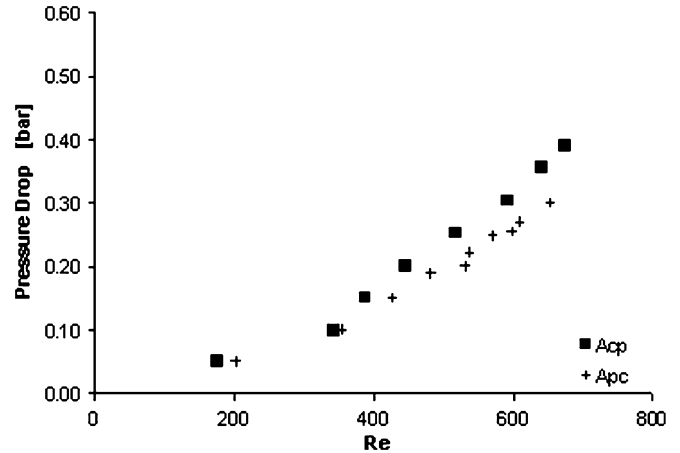
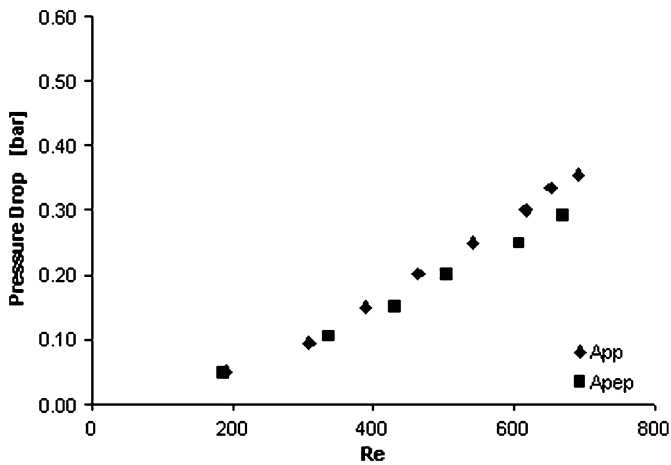
Fig. 12. Pressure drops of the pair Apc and Apec versus Re number.

Fig. 14. Pressure drops comparison of the pairs Acp and Apc.

Fig. 13. Pressure drops of the pair App and Apep versus Re number.

2001) assuming that the flow distribution is uniform and laminar regime:

$$\Delta p = \xi \rho \frac{v^2}{2}, \quad (17)$$

with

$$\xi = f_i \frac{l}{d} = \frac{64}{Re} \frac{l}{d}. \quad (18)$$

These values are too small to be observed compared with the total pressure drops of the tested model; this is compatible with the experimental results.

The assembly App without the MCHE connected shows a greater pressure drop than Apep that includes the MCHE. The difference between these two increases with Re and the maximum is about 20.6%, corresponding to a Re of 670. It might be explained as follows. Compared to other pairs, the flow distribution in the pair App and Apep is the most nonuniform. And the installation of the MCHE between two conventional pyramid distributors changes the flow pattern both in the distributors and in the MCHE which, to some extent, weakens the effects

of eddy flow, disturbance and flushing existing in the distributors and leads to a lower pressure drop. This explanation needs to be confirmed under a wider condition range.

An interesting feature is that the pressure drop of Apec is smaller than that of Acp. It is a typical *nonsymmetrical phenomenon*, that is to say, the flow pattern and governed mechanics are not the same when the constructal component functions as the inlet distributor or outlet collector integrated to a heat exchanger. Comparing two pairs Acp and Apc independently, without considering the effect of MCHE, the difference is clear (about 20% for a Re of 650), as shown in Fig. 14. The fluid movements for sudden expansion and sudden contraction are not the same, as more vortices would be generated in the former case. This would be verified with the simulated results of fluid dynamic analysis in the next section.

Now, let us turn back to the thermal performance analysis and recall the result that it is the Apec that has the best thermal performance among all of the tested configurations, even better than Acec. Relatively better thermal performance associated with low pressure drop at the same time, it seems that the assembly configuration Apec with a conventional pyramid inlet distributor and a constructal outlet collector is the best mode under our considered conditions.

5. Fluid dynamic analysis

In the view point of fluid dynamics, the behaviors of the flowing fluid inside the distributor/collector configurations described in the previous sections are rather complex as it may be far from an ideal fluid due to the strong influence of inner structure boundaries. In the experimental system, three types of boundary influences can be identified:

- Sudden changes of flowing directions in the constructal distributor (tee-type joints and 90° elbows).
- Sudden expansions/contraction at the inlet/outlet mouths of the tubes of the constructal distributor, collector as well as the MCHE.
- Expansion or contraction in the pyramid-shaped channels.

In general, any change of fluid velocity, in either direction or magnitude, can generate vortices that develop when normal streamlines are disturbed and when boundary layer separation occurs. The vortices are kept in motion by the shear stresses between them and the separated current and consume considerable mechanical energy, and then may lead to loss of pressure in the fluid. The energy loss resulting from the vortices formation due to the boundary changes is also interpreted as an additional friction, called form friction. In our

cases, the analysis in Figs. 10–13 indicate that the skin friction resulting from flow through the MCHE is neglectable compared to the form frictions, which control the resistances in all the cases.

5.1. Resistance in the constructal distributor

To investigate the resistance in a constructal distributor, CFD (computational fluid dynamics) simulations were performed by using the model structure given in Fig. 15. For simplifying the simulation, the model structure corresponds to a half part of the real constructal structure used in the experiments.

A CFD model that can consider fluid viscosity and shear stress is used by implementing it into the commercial code FLUENT for the simulation. The computed velocity contours on different cross sections of the first and third layers, and their sub-branches are shown in Fig. 16. The colors represent the magnitude and the arrowheaded lines represent the directions of the velocities. As shown in Fig. 16(a), vortices develop at the immediate downstream of the first tee joint where the fluid comes into the first layer and is forced to change its velocity direction. With the turbulence, when the fluid changes again its direction by passing through tee joint 2 and comes to section A2, even stronger vortices can be observed. This is shown in Fig. 16(b). The simulating results demonstrate that the fluid

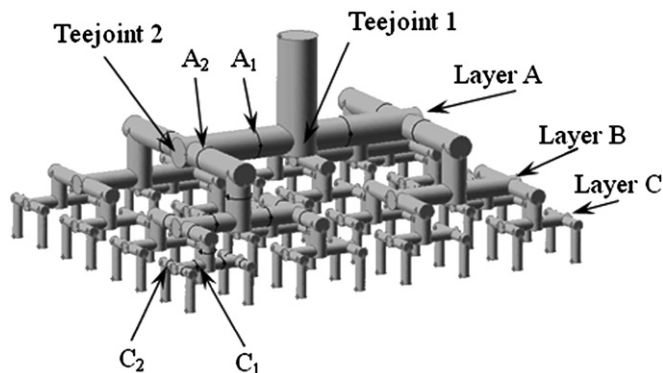


Fig. 15. The model structure for CFD simulation for the constructal distributor.

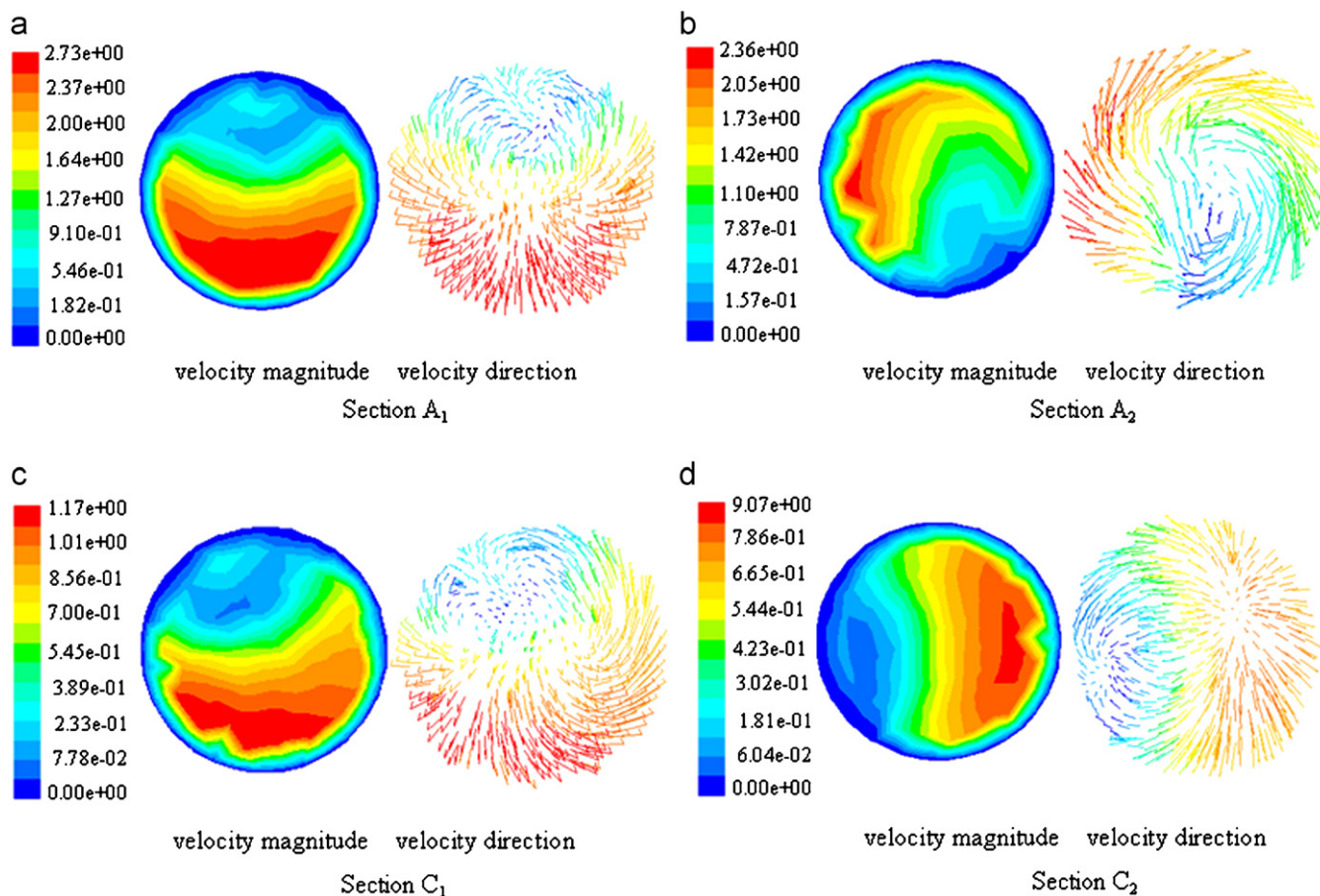


Fig. 16. Contours for velocity magnitude and vectorial velocity on tube sections of the constructal distributor (Re for the lowest level tube: 737).

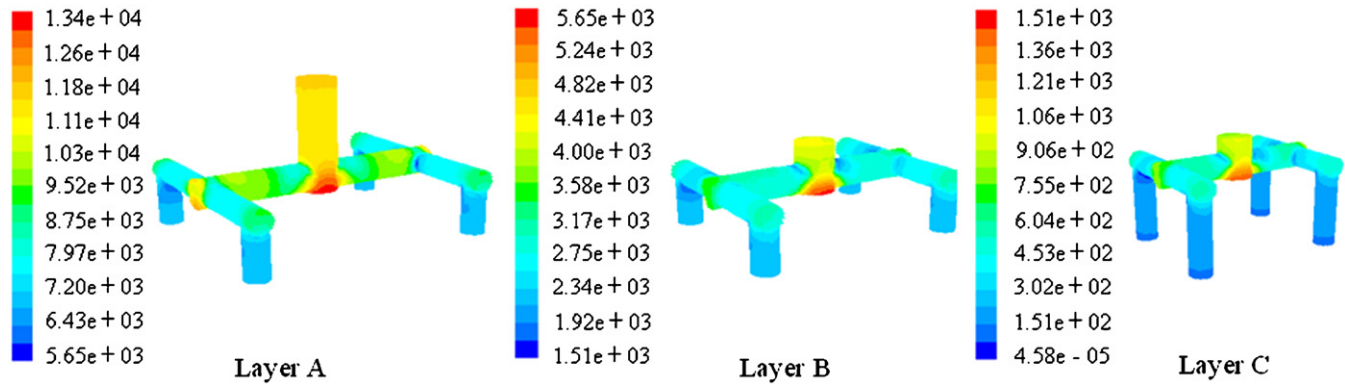


Fig. 17. Pressure distribution on the constructal distributor (Re for the lowest level tube: 737).

flow at the outlets of all the tee joints has the similar pattern as shown in Fig. 16(a) and (b). Fig. 16(c) and (d) show the cases for sections C1 and C2. Comparing Fig. 16(c) with (a), it can be seen that the flowing pattern at section C1 is no longer symmetric as that at section A1, and this is because the fluid enters the Layer C with its vortices that has developed at upper level tee joints or elbows.

The flowing resistance generated by the vortices can also be found by observing the pressure distribution as shown in Fig. 17. It can be seen that the violent changes in colors are all concentrated at the locations of tee joints and the elbows. This suggests that *the frictions from the skin of tubes are small or neglectable compared to the form frictions*.

In fact, the resistance estimations of pipe fits like tee joint and elbow have been well established. This is usually done by introducing a proper resistance factor ζ_f in an equation with the form of Eq. (17). However, the available factors for use have been developed by assuming a sufficiently developed turbulent flow in a straight tube. Fig. 16 demonstrates that, because the lengths of the straight tubes in the constructal distributor are far from sufficient for a full developed turbulent flow, the flowing patterns at different locations are integrated, and the resistance depends strongly on the constructal geometry.

In an elbow or T one can suppose that ζ is constant as soon as $Re > 500$. If it is not turbulent, we generally pose

$$\zeta = \zeta_t + \frac{\zeta_l}{Re}, \quad (19)$$

where ζ_t is the turbulent coefficient and ζ_l is a coefficient suitable for the stokesian mode (Re to 0). These coefficients apply only for one isolated singularity. For two successive elbows nonseparated by at least 10–20 diameters ζ total is not the sum of ζ individual. Therefore in each configuration it is necessary to determine ζ . In addition, this ζ depends on the exact conformation of the singularity. Two elbows connection in S type or U type do not present the same one because of the orientation compared to the vector g ; the same problem will exist as they are assembled vertically or horizontally. The digital simulation highlights these effects well.

5.2. Resistance of the distributor/collector systems

Fig. 14 has shown that the configuration defined by Apc gives lower pressure drop than Acp that has the same geometry structure but with opposite flowing direction of the fluid. This can be explained by the fact that *the form friction for sudden expansion is greater than that generated by sudden contraction*. The former, if represented by the form of Eq. (17), corresponds a resistant factor ζ_e with the value of 1, yet the resistant factor ζ_c for the latter has a value of 0.4–0.5 (Hewitt, 1992). The estimations of these values have been based on the assumption that the flowing regime (laminar or turbulent) dose not change before and after the expansion or contraction, and is confined in straight tubes with sudden change in inner diameter. In the cases of the constructal distributor/collector configurations, instead of a large size regular tube, the fluid expands to or contracts from a pyramid-shaped channel, which may lead to the generation of an additional form resistance. On the other hand, for the Acp configuration, *the vortices generated by the fluid coming out from one individual small tube to the pyramid channel can interact with those generated by the sudden expansion of fluid coming from other tubes*. This may generate additional eddies and associated frictions.

Fig. 18 is the model structure we used in our CFD simulation for investigating the resistance behaviors for the distributor configurations. With the symmetric assumption, a quarter of the distributor system is adopted as the model, and the similar geometrical form is kept but with less number of layers of the constructal distributor, for the purposes of simplification (to avoid computational burden). With the same flow rate of the fluid (same Re number), we assume that the resistances in the tubes of constructal distributor and of the MCHE do not change for different configurations, and the difference in the pressure drop for the different configurations is mainly due to the difference among the form resistances generated by the different geometrical configurations. Table 2 gives the simulated results of the pressure drops. Differences in the resistances for the Apc and Acp configurations can be observed in the table. Fig. 19 shows the flow patterns in the distributor/collector configurations of Apc and Acp. More vortices can be observed in the

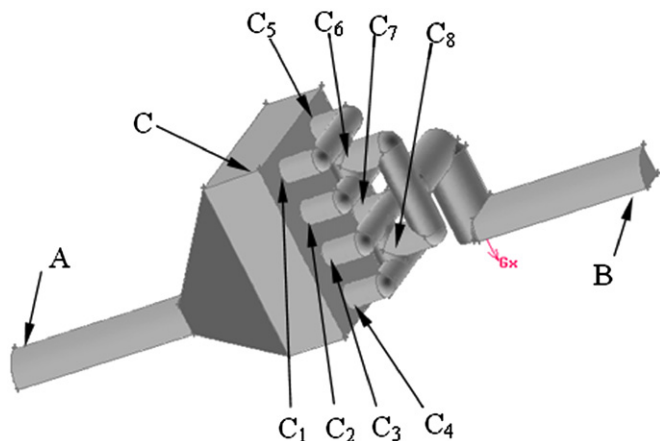


Fig. 18. Model structure used in CFD simulation.

Table 2
Simulated results in pressure drops for Apc and Acp configurations

Re	Configuration	Δp total (kPa)	Δp in pyramid (kPa)
1468	Apc	12.05	1.179
	Acp	16.02	4.81
520	Apc	1.7	0.165
	Acp	2.05	0.69

case of Acp where the fluid goes through sudden expansions. This is consistent with our experimental results conducted in the previous sections.

It should be pointed out that the values of pressure drop reported were taken from the pressure values in average over the corresponding cross sections. An explicit analysis on the

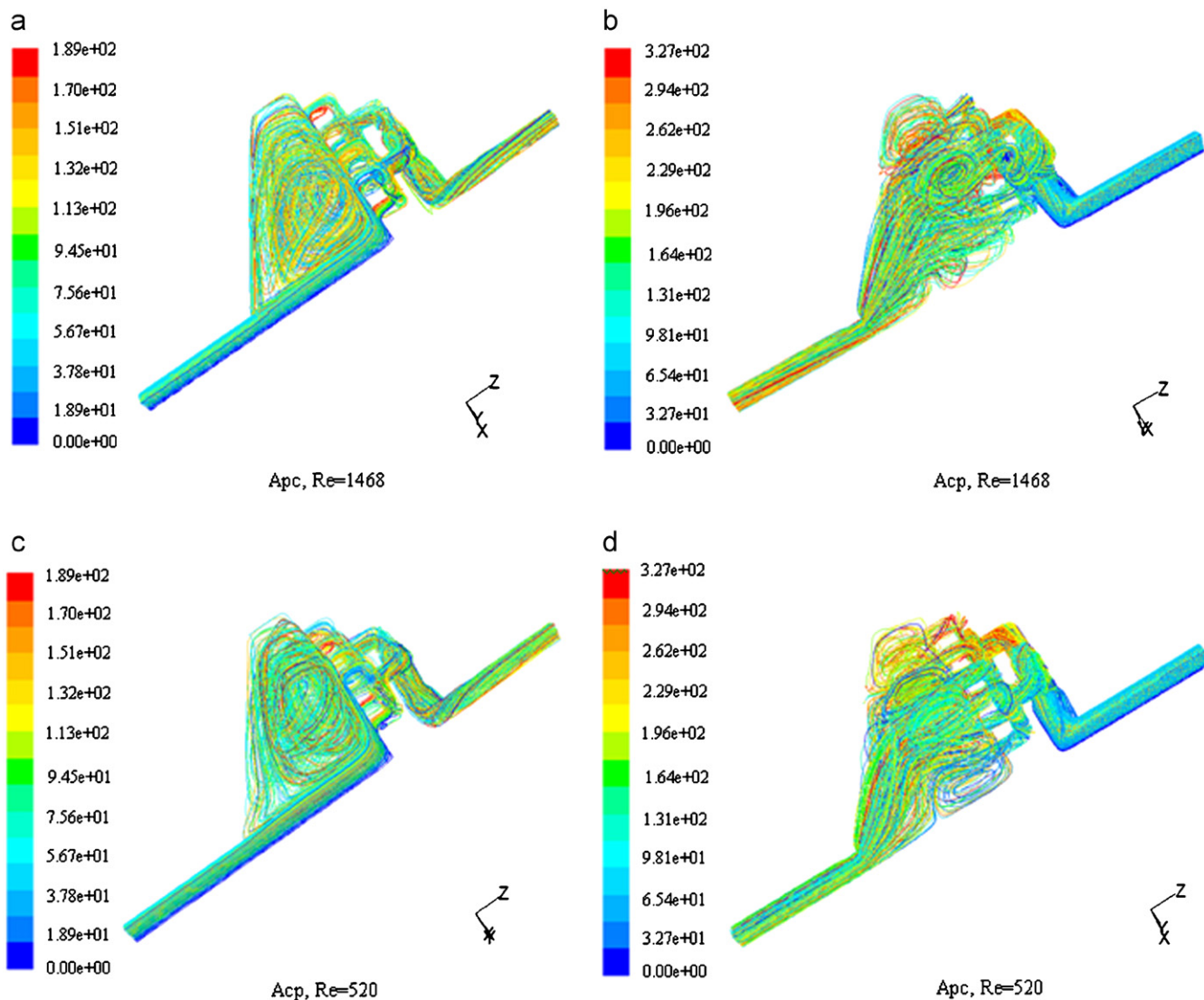


Fig. 19. Flow patterns in the distributor/collector configurations of Apc and Acp.

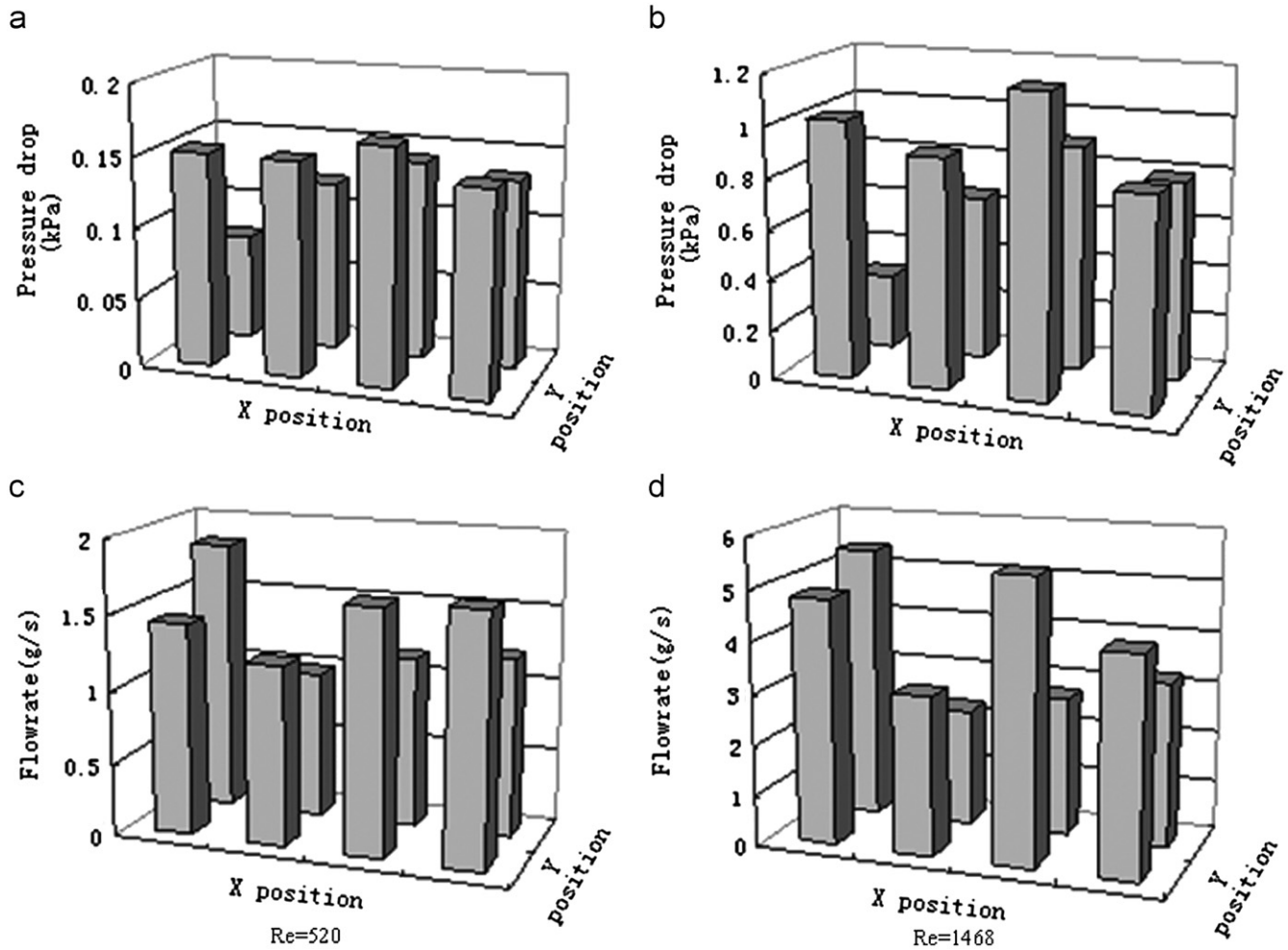


Fig. 20. Simulated results on the pressure distribution at the joint sections and the flowrate distribution among the tubes for the case of Apc.

pressure distribution is difficult because of the complex fluid flow phenomena within the zone of the vortices. The difficulty also comes from the interaction between the effect of the pyramid and that of the constructal geometries. Even though the symmetric nature can guarantee the same resistances for each channels of the constructal distributor, the uneven distribution in fluid flow in the pyramid channel may exert different pressures at different locations on cross section C where the mouths of the tubes of the constructal distributor are located, and lead to different flow rate in the tube. The differences in flow rate in the tubes in turn generate difference in their resistances. Fig. 20 gives the simulated results on the pressure distribution at the joint sections of the tubes with the pyramid and the flow rate distribution among the tubes of the lowest level layer of the constructal collector for the case of Apc. Note that the values of the pressures in Fig. 20 are the pressure drops from point A to each of the corresponding joint sections.

It should be also pointed out that the analysis with the CFD simulation is preferably valid only for the specific cases in our investigation. The flow patterns in such a complex boundary geometry depend heavily on the size and shape of the structure, and also on the flow rate as well as physical property of the fluid.

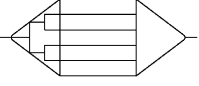
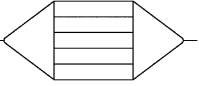
So, in-depth investigations on the quantity characterization of the fluid dynamics of the system are needed.

6. Assembly configuration optimization

From both experimental and simulation results discussed above, it could be concluded that thermal performance and pressure drop of different assembly configurations could be very different. In fact, it is not the Acec, which is supposed to ensure the most uniform flow distribution in the core of the MCHE, that has the best thermal performance. The Apec with a conventional pyramid inlet distributor and a constructal outlet collector performs better than other three assembly configurations: Acep, Acec and Apec, with the overall heat transfer coefficient and pressure drop considered. In this part, we try to get relationship that amounts to the bridging of the gaps between thermal performances; flow distribution and pressure drop for assembly configuration optimization.

Let us first make a fine investigation of the pressure drop. The pressure drop measured or simulated is that of the entire assembly (given the name of Δp_{total}), which is the sum of the pressure drops in distributor, heat exchanger and collector

Table 3
Synthesis of flow distribution and pressure drop for assembly configuration optimization

Assembly configuration	Flow distribution	$\Delta p_e/\Delta p_{\text{total}}$	U
Acep 	Good	Low	High
Apec 	Very good	High	Very high
Acec 	Excellent	Very low	High
Apep 	Bad	High	Low

(given the names of Δp_d , Δp_e and Δp_c , respectively).

$$\Delta p_{\text{total}} = \Delta p_d + \Delta p_e + \Delta p_c. \quad (20)$$

Δp_d and Δp_c signify energy losses of dissipation, whereas Δp_e corresponds to flow rate and Re in the core of heat exchanger, which means the useful pressure drop for heat transfer. For a high heat exchange performance (high overall heat transfer coefficient U), two criteria should be satisfied:

- uniform flow distribution
- relatively high Δp_e .

In other words, for a total pressure drop Δp_{total} given, the pressure drops contributed by distributor and collector (Δp_d and Δp_c) should be as little as possible to have a relative high ratio of $\Delta p_e/\Delta p_{\text{total}}$, and the flow distribution should be as uniform as possible. These two criteria reveal the conflict that accompanies the integration of constructal distributor/collector to the MCHE: the constructal component, which could improve the quality of flow distribution, also result in higher energy losses of dissipation. As a result, a compromise between these two dominant mechanisms should be made to find an optimal assembly configuration.

Reconsidering the distribution quality, the pressure drops of four different assembly configurations, as shown in Table 3, we could reach the conclusion that the assembly with conventional pyramid inlet distributor and constructal outlet collector (Apec) can achieve optimum thermal performance of the MCHE by combining uniform flow distribution with small pressure drop of dissipation. Acep is the second best choice as it has almost equal thermal performance as that of the Acec but obviously consumes less driving power in our cases.

The fact that Apec performs better than Acec has been proved by both experimental and simulation results. In a sense, it is not only valid in our cases, but it might be a widespread phenomenon accompanying with *nonsymmetrical problems*. Similar proofs in various other industry processes need to be found

and deterministic theoretical breakthrough should also be useful for a more quantitative explanation. Our hope is that this will lead to more effective interactions between the various sections of the field, and certainly, to a broader and more explicit view of the phenomena.

7. Conclusion

This paper deals with the novel idea of coupling constructal distributors/collectors with a heat exchanger in order to solve the problem of flow maldistribution and then lead to its thermal performance improvement. The design procedure and scaling laws of constructal distributor have been introduced briefly. Experimental and simulation analysis have been done to investigate relations among flow distribution, heat transfer and pressure drop. Different assembly configurations involving distributor, collector and heat exchanger have also been compared. Based on the discussion above, the following conclusions could be reached.

- The constructal distributor/collector can to some extent satisfy the need of fluid equidistribution and consequently lead to the thermal performance improvement of the MCHE. The overall heat transfer coefficients of Acec and Acep are about from 30% to 15% higher than that of the Apep on our experimental conditions depending on flow rate, and more encouraging performance (28% higher) could be achieved by using Apec. The improvement is significant even with the uncertainty considered and all these results highlight heat transfer intensification on laminar flow by constructal theory.
- Higher pressure drops are also induced due to the strong influence of inner structure boundaries in constructal distributor. Sudden changes of directions and sudden expansions/contractions along the tubes of constructal distributor induce vortices, which consume considerable mechanical energy and lead to loss of pressures in the fluid. The pressure drop of Acec is 72.4% higher than that of Apep at maximum condition. The pressure drop resulting from flow through the MCHE is neglectable compared to the total pressure drop of the assembly.
- It is also observed that additional eddies and associated frictions for sudden expansion is greater than that generated by sudden contraction, since the vortices generated by the fluid coming out from one individual small tube to the pyramid channel can interact with those generated by the sudden expansion of fluid coming from other tubes. As a result, among all tested assembly configurations, Apec has shown a relatively uniform flow distribution as well as low pressure drop for dissipation at the same time under our considered conditions, which leads to a better thermal performance. It is surely the optimal configuration in our cases.

The analysis with experiment and CFD simulation is limited in low Reynolds number conditions and is preferably valid for the specific cases in our investigation. As already noted above, in-depth investigations on the quantity characterization of the fluid dynamics of the system are needed and the domain of

turbulent flow pattern should be explored to find more general conclusions.

Finally, for “hot” heat exchangers or relatively high pressure work, polymer materials are obviously inadequate. Metallic distributors that have been recently fabricated (using direct metal powder stereolithography) will allow the test involving a large range of temperature and flow rate. CFD models that can deal with large eddies and PIV visualized method are in developing. All the above studies will ultimately furnish guidelines for the design of more performing distributors.

Notation

A	heat transfer surface, m^2 ; assembly
d	diameter of channel, m
D_k	viscous dissipation power in all channels of scale k , W
f_i	friction coefficient, dimensionless
f_k	flow rate in a channel of scale k , m^3/s
f_0	total flow rate into and out of the construct, m^3/s
F	LMTD correction factor, dimensionless
h	heat transfer coefficient for one fluid, $W/m^2 K$
k	index of generation or scale; thermal conductivity, $W/m K$
l	length of the heat exchanger channel, m
L	length of the side of the square construct, m
m	total number of generations or scales, dimensionless
n	number of the channels on one face of the MCHE
n_k	number of channels in scale k , dimensionless
N	number of points (outlet ports), dimensionless
Nu	Nusselt number
Δp	pressure drop, bar
Pr	Prandtl number
q	heat transfer, W
r_k	radius of channel of scale k , m
Re	Reynolds number
T	temperature, $^{\circ}C$
U	overall heat transfer coefficient, $W/m^2 K$

Greek symbols

β	surface area density, m^2/m^3
δ	thickness, m
ζ	expansion-loss coefficient, dimensionless
ξ	resistance factor, dimensionless
μ	viscosity, $kg/m s$
μ_w	viscosity in wall temperature, $kg/m s$
v	velocity in the channel of heat exchanger, m/s

Subscripts

c	constructal distributor
cold	cold fluid
e	mini crossflow heat exchanger (MCHE)
hot	hot fluid
in	inlet

k	scale number
out	outlet
p	conventional pyramid distributor

Acknowledgments

This work is supported by the French ANR (Agence Nationale de la Recherche) within the “programme non thématique 2005, Projet no. NT05-3_41570). One of the authors, L. Luo, would like to thank Dr. A. Bejan, for his fruitful discussions and helpful suggestions.

References

- Aganda, A.A., Coney, J.E.R., Farrant, P.E., Sheppard, C.G.W., Wongwuttanasatian, T., 2000. A comparison of the predicted and experimental heat transfer performance of a finned tube evaporator. *Applied Thermal Engineering* 20, 499–513.
- Ahern, J.E., 1980. *The Exergy Method of Energy Systems Analysis*. Wiley, New York.
- André, J.C., Corbel, S., (Collective) 1994. *Stéréolithographie Laser*. Polytechnica, Paris, ISBN 2-084254-021-5.
- Bejan, A., 1997. Constructal theory network of conducting paths for cooling a heat generating volume. *International Journal of Heat and Mass Transfer* 40, 799–811.
- Bejan, A., 2000a. From heat transfer principles to shape and structure in Nature: constructal theory. *Journal of Heat Transfer. Transactions of the ASME* 122, 430–449.
- Bejan, A., 2000b. *Shape and Structure, from Engineering to Nature*. Cambridge University Press, UK, p. 344.
- Bejan, A., Tondeur, D., 1998. Equipartition, optimal allocation, and the constructal approach to predicting organization in Nature. *Revue Générale de Thermique* 37, 165–180.
- Bobbili, P.R., Kumar, P.K., Das, S.K., 2002. Effect of flow distribution to the channels on the thermal performance of a plate heat exchanger. *Chemical Engineering and Processing* 41, 49–58.
- Bobbili, P.R., Sundén, B., Das, S.K., 2006. An experimental investigation of the port flow maldistribution in small and large plate package heat exchangers. *Applied Thermal Engineering* 26, 1919–1926.
- Chiou, J.P., 1978. Thermal performance deterioration in crossflow heat exchanger due to the flow nonuniformity. *ASME Journal of Heat Transfer* 100, 580–587.
- Chiou, J.P., 1980. The advancement of compact heat exchanger theory considering the effects of longitudinal heat conduction and flow nonuniformity effects. In: Shah, R.K., McDonald, C.F., Howards, C.P. (Eds.), *Compact Heat Exchangers-Mechanical Engineering-History, Technological Advancement and Mechanical Design Problems*. ASME, New York, pp. 101–121.
- Fleming, R.B., 1967. The effect of flow distribution in parallel channels of counter-flow heat exchangers. *Advances in Cryogenic Engineering* 12, 352.
- Gut, J.A.W., Fernandes, R., Pinto, J.M., Tadini, C.C., 2004. Thermal model validation of plate heat exchangers with generalized configurations. *Chemical Engineering Science* 59, 4591–4600.
- Hewitt, G.F., 1992. *Handbook of Heat Exchanger Design*. Begell House, New York.
- Holman, J.P., 2001. *Heat Transfer*. McGraw-Hill Ed.9, New York, ISBN 0-07-240655-0.
- Jiao, A., Baek, S., 2005. Effects of distributor configuration on flow maldistribution in plate-fin heat exchangers. *Heat Transfer Engineering* 26, 19–25.
- Jiao, A., Zhang, R., Jeong, S.K., 2003. Experimental investigation of header configuration on flow maldistribution in plate-fin heat exchanger. *Applied Thermal Engineering* 23, 1235–1246.
- Lalot, S., Florent, P., Lang, S.K., Bergles, A.E., 1999. Flow maldistribution in heat exchangers. *Applied Thermal Engineering* 19, 847–863.

- Luo, L., Tondeur, D., 2005a. Optimal distribution of viscous dissipation in a multi-scale branched fluid distributor. *International Journal of Thermal Sciences* 44, 1131–1141.
- Luo, L., Tondeur, D., 2005b. Multiscale optimisation of flow distribution by constructal approach. *China Particuology* 3, 329–336.
- Luo, L., D'ortona, U., Tondeur, D., 2000. Compact Heat Exchangers. In: Ehrfeld, W. (Ed.), *Microreaction Technology: Industrial Prospects*. Springer, Berlin, pp. 556–565.
- Luo, L., Hoareau, B., D'ortona, U., Tondeur, D., Legall, H., Corbel, S., 2001. Design, fabrication and experimental study of new compact mini heat-exchangers. IMRET5—5th International Conference on Microreaction Technology, Strasbourg.
- Luo, L., Tondeur, D., Le Gall, H., Corbel, S., 2006. Constructal approach and multi-scale components. *Applied Thermal Engineering* 27, 1708–1714.
- Luo, X., Roetzel, W., 1998. Theoretical investigation on cross-flow heat exchangers with axial dispersion in one fluid. *Revue Générale de Thermique* 37, 223–233.
- Luo, X., Roetzel, W., 2001. The single-blow transient testing technique for plate-fin heat exchangers. *International Journal of Heat and Mass Transfer* 44, 3745–3753.
- Mueller, A.C., Chiou, J.P., 1988. Review of various types of flow maldistribution in heat exchangers. *Heat Transfer Engineering* 9, 36–50.
- Ranganayakulu, Ch., Seetharamu, K.N., 1999a. The combined effects of longitudinal heat conduction, flow nonuniformity and temperature nonuniformity in crossflow plate-fin heat exchangers. *International Communications in Heat and Mass Transfer* 26, 669–678.
- Ranganayakulu, Ch., Seetharamu, K.N., 1999b. The combined effects of wall longitudinal heat conduction, inlet fluid flow nonuniformity and temperature nonuniformity in compact tube-fin heat exchangers: a finite element method. *International Journal of Heat and Mass Transfer* 42, 263–273.
- Roetzel, W., Das, S.K., 1995. Hyperbolic axial dispersion model: concept and its application to a plate heat exchanger. *International Journal of Heat and Mass Transfer* 38, 3065–3076.
- Roetzel, W., Ranong, C.N., 1999. Consideration of maldistribution in heat exchangers using the hyperbolic dispersion model. *Chemical Engineering and Processing* 38, 675–681.
- Sahoo, R.K., Roetzel, W., 2002. Hyperbolic axial dispersion model for heat exchangers. *International Journal of Heat and Mass Transfer* 45, 1261–1270.
- Seider, E.M., Tate, C.E., 1936. Heat transfer and pressure drop of liquids in tubes. *Industrial and Engineering Chemistry* 28, 1429–1435.
- Srihari, N., Bobbili, P.R., Sunden, B., Das, S.K., 2005. Transient response of plate heat exchangers considering effect of flow maldistribution. *International Journal of Heat and Mass Transfer* 48, 3231–3243.
- Tondeur, D., Luo, L., 2004. Design and scaling laws of ramified fluid distributors by the constructal approach. *Chemical Engineering Science* 59, 1799–1813.
- Wen, J., Li, Y., 2004. Study of flow distribution and its improvement on the header of plate-fin heat exchanger. *Cryogenics* 44, 823–831.
- Wen, J., Li, Y., Zhou, A., Zhang, K., 2006. An experimental and numerical investigation of flow patterns in the entrance of plate-fin heat exchanger. *International Journal of Heat and Mass Transfer* 49, 1667–1678.
- Xuan, Y., Roetzel, W., 1993. Stationary and dynamic simulation of multipass shell and tube heat exchangers with the dispersion model for both fluids. *International Journal of Heat and Mass Transfer* 36, 4221–4231.
- Yuan, P., 2003. Effect of inlet flow maldistribution on the thermal performance of a three-fluid crossflow heat exchanger. *International Journal of Heat and Mass Transfer* 46, 3777–3787.